Journal of Hazardous Materials 195 (2011) 291–297

Contents lists available at SciVerse ScienceDirect

Journal of Hazardous Materials

journal homepage: www.elsevier.com/locate/jhazmat

# Tantalum (oxy)nitrides: Preparation, characterisation and enhancement of photo-Fenton-like degradation of atrazine under visible light

Yingxun Du*, Lu Zhao, Yaling Su

*Nanjing Institute of Geography and Limnology, State Key Laboratory of Lake Science and Environment, Chinese Academy of Sciences, Nanjing 210008, China*

ARTICLE INFO

*Article history:*
Received 22 May 2011
Received in revised form 16 July 2011
Accepted 13 August 2011
Available online 22 August 2011

*Keywords:*
Tantalum (oxy)nitrides
Photo-Fenton-like
$Fe^{3+}$ reduction
Visible light
Atrazine

ABSTRACT

Tantalum (oxy)nitrides were prepared by the nitridation of $Ta_2O_5$ and were added to a photo-Fenton-like system to enhance $Fe^{3+}$ reduction and atrazine degradation under visible light. The samples were characterized by XRD, XPS, DRS and BET analyses. XPS analysis showed that the nitrogen content of the tantalum (oxy)nitride samples increased noticeably with the nitridation temperature and nitridation time but slightly with the flow rate of $NH_3$. XRD results showed $Ta_2O_5$ was first converted to TaON and then to $Ta_3N_5$ when the nitridation temperature increased. DRS analysis showed that the sample obtained at 800 °C displayed the strongest absorption of visible light. However, the ability of the tantalum (oxy)nitrides to reduce $Fe^{3+}$ did not increase continuously with the nitrogen content. Sample 7 (700 °C, $Q_{NH_3}$ = 0.3 L/ min, 6 h) showed the highest level of photocatalytic activity for $Fe^{3+}$ reduction. This is because the photocatalytic activity of TaON for $Fe^{3+}$ reduction is higher than that of $Ta_3N_5$. And a slight synergetic effect was observed between TaON and $Ta_3N_5$. With the addition of sample 7, $H_2O_2$ decomposition and atrazine degradation were significantly accelerated in a photo-Fenton-like system under visible light. The regenerated tantalum (oxy)nitrides catalyst displayed considerably stable performance for atrazine degradation.



## 1. Introduction

The photo-Fenton-like ($Fe^{3+}/H_2O_2$) and photo-Fenton ($Fe^{2+}/H_2O_2$) systems constitutes one kind of the most attractive advanced oxidation processes, as the materials required are relatively abundant, inexpensive, and environmentally benign. In photo-Fenton-like and photo-Fenton system, the degradation of the contaminant is based on the attack of the active hydroxyl radical (•OH), which is generated by the reaction of $Fe^{2+}$ and $H_2O_2$ (Eqs. (1) and (2)). A variety of refractory organics such as chlorinated phenols, herbicides and dyes can be decomposed effectively by the photo-Fenton(-like) reactions [1–6].

In photo-Fenton(-like) reaction, the cycling of the catalyst ($Fe^{2+}/Fe^{3+}$) is key to the effective degradation of the contaminant. Eqs. (1) and (3) showed the cycling of iron ions driven by $H_2O_2$. $Fe^{2+}$ is oxidized by $H_2O_2$ with a high rate constant. But the reduction of $Fe^{3+}$ by $H_2O_2$ is slow and thus ineffective. In photo-Fenton(-like)processes, the efficient way to reduce $Fe^{3+}$ is the irradiation of UV light ($\lambda < 360$ nm) (Eq. (4)) [7]. However, the industrial applicability of this process is limited since natural UV comprises only 3–5% of the solar light energy that reaches the earth.

$$Fe^{2+} + H_2O_2 \rightarrow Fe^{3+} + {}^{\bullet}OH + OH^- \quad k_1 = 51\,M^{-1}\,s^{-1}[8] \tag{1}$$

$$^{\bullet}OH + P \xrightarrow{k_{^{\bullet}OH}} \text{intermediates} \tag{2}$$

$$Fe^{3+} + H_2O_2 \rightarrow Fe^{2+} + HO_2^{\bullet} + H^+ \quad k_3 = 0.001\text{–}0.01\,M^{-1}\,s^{-1}[9] \tag{3}$$

$$Fe(OH)^{2+} \xrightarrow{h\nu} Fe^{2+} + {}^{\bullet}OH \tag{4}$$

Many semiconductor compounds, especially $TiO_2$ have been used as the photocatalysts in the reactions driven by solar energy such as water splitting and photocatalytic degradation [10–13]. The modified $TiO_2$ such as metal-doped or/and nonmetal-doped $TiO_2$ possessed the photocatalytic activity under visible light [12,14–18].

Tantalum (oxy)nitrides ($Ta_3N_5$ and TaON) have narrow band gaps of 2.08 and 2.4 eV [19], respectively, making them suitable as visible-light driven photocatalysts. With respect to the modified $TiO_2$ such as Ce–N codoped $TiO_2$, C–N codoped $TiO_2$ and bimetal codoped (Bi-Co and Fe-Co) $TiO_2$ [12,15,17], $Ta_3N_5$ and TaON have relatively simple composition and structure. It has been found that TaON and $Ta_3N_5$ were novel photocatalysts suitable for water decomposition and pollutant degradation reactions driven by visible light [20–22]. Compared with $TiO_{2-x}N_x$ in the same size, $Ta_3N_5$

* Corresponding author. Tel.: +86 025 86882116; fax: +86 025 57714759.
*E-mail address:* yxdu@niglas.ac.cn (Y. Du).

0304-3894/$ – see front matter © 2011 Elsevier B.V. All rights reserved.
doi:10.1016/j.jhazmat.2011.08.042

**Table 1**
Composition, BET surface area and the ability to reduce $Fe^{3+}$ of the tantalum (oxy)nitride samples prepared under various conditions.

| No. | Conditions | Ta:O:N | Specific surface area ($m^2$/g) | $Fe^{2+}$ (mg/L) | Reduction of $Fe^{3+}$ (%) |
|---|---|---|---|---|---|
| 1 | 600 °C, 0.1 L/min, 6 h | 1:3.0:0.10 | 0.896 | 0.129 | 0.45 |
| 2 | 600 °C, 0.5 L/min, 6 h | 1:2.67:0.26 | 1.000 | 0.317 | 1.12 |
| 3 | 600 °C, 0.3 L/min, 6 h | 1:2.62:0.34 | 1.548 | 0.534 | 1.90 |
| 4 | 700 °C, 0.1 L/min, 6 h | 1:2.18:0.66 | 9.014 | 1.489 | 5.31 |
| 5 | 700 °C, 0.3 L/min, 2 h | 1:3.32:0.24 | 1.894 | 0.425 | 1.51 |
| 6 | 700 °C, 0.3 L/min, 4 h | 1:2.0:0.86 | 9.796 | 1.737 | 6.19 |
| 7 | 700 °C, 0.3 L/min, 6 h | 1:1.86:0.80 | 14.25 | 2.003 | 7.15 |
| 8 | 800 °C, 0.3 L/min, 2 h | 1:1.88:0.94 | 9.433 | 1.586 | 5.65 |
| 9 | 800 °C, 0.3 L/min, 6 h | 1:1.50:1.07 | 8.549 | 1.171 | 4.17 |
| 10 | 800 °C, 0.1 L/min, 6 h | 1:1.44:1.03 | 9.656 | 1.320 | 4.70 |
| 11 | 800 °C, 0.5 L/min, 6 h | 1:1.16:1.17 | 9.654 | 0.700 | 2.50 |

showed much higher photocatalytic activity for the degradation of methylene blue under visible light irradiation [20]. To improve the efficiency of photo-Fenton system under visible light irradiation, Wang et al. [23] introduced $Ta_3N_5$ into the photo-Fenton system and found that $Ta_3N_5$ was effective to promote the reduction of $Fe^{3+}$ under visible light and thus the degradation of N,N-dimethylaniline and 2,4-dichlorophenol. The mechanism of iron ions cycling in the presence of $Ta_3N_5$ was also proposed. Under visible light, $Ta_3N_5$ is excited to form electrons in the conduction band and holes in the valence band. The photoelectrons are captured by $Fe^{3+}$ to generate $Fe^{2+}$, while the generated $Fe^{2+}$ is oxidized by $H_2O_2$ immediately to regenerate $Fe^{3+}$ and thus a rapid iron ions cycling is established.

Tantalum (oxy)nitrides are usually obtained by the nitridation of $Ta_2O_5$ in a $NH_3$ flow. The nitridation reaction always leads to the formation of a mixture of TaON and $Ta_3N_5$ [19]. The composition of the prepared sample was affected by the nitridation temperature, the nitridation time and the flow rate of $NH_3$. Thus, the preparation condition should influence the photocatalytic activity of the samples. However, to the best of our knowledge, little information on the photocatalytic activity for $Fe^{3+}$ reduction of the samples prepared under various conditions is available.

In this study, the tantalum (oxy)nitride samples were prepared by the nitridation of $Ta_2O_5$ at first. XPS and DRS analysis showed that increasing the nitridation temperature, the nitridation time and the flow rate of $NH_3$ led to the higher content of nitrogen and the stronger absorption of visible light. But it was interesting to find that the photocatalytic activity for $Fe^{3+}$ reduction is not increased continuously with the nitrogen content. This is because the photocatalytic activity of TaON for $Fe^{3+}$ reduction is higher than that of $Ta_3N_5$, confirmed by the experimental data. And a slight synergetic effect was observed between TaON and $Ta_3N_5$. In the photo-Fenton-like system under visible light, the degradation of atrazine was significantly accelerated by the tantalum (oxy)nitrides sample. And the regenerated catalyst was considerably stable for atrazine degradation.

## 2. Experimental

### 2.1. Materials

$Ta_2O_5$, $Fe_2(SO_4)_3$ and hydrogen peroxide (30%) were purchased from Sinopharm Chemical Reagent Co., Ltd., China. $NH_3$ (99.99%) was supplied by Special Gas Co., Ltd., Nanjing, China. Atrazine was from Tokyo Chemical Industry Co., Ltd., Japan. Deionized water was used throughout this study.

### 2.2. Preparation and characterisation of tantalum (oxy)nitrides

For the preparation of tantalum (oxy)nitrides, 2.0 g of $Ta_2O_5$ was put into a quartz tube, which was put into a tube furnace and then subjected to nitridation under a flow of $NH_3$ at rates ranging from 0.1 to 0.5 L/min. The nitridation temperature ranged from 600 to 800 °C, and the nitridation time was 2–6 h. After the reaction, the sample was cooled to room temperature in the flow of $N_2$. The detailed conditions for the preparation of each sample are summarized in Table 1.

The phase composition of the sample was characterized by X-ray diffraction (XRD) (model D/max-rA, Rigaku Co., Tokyo, Japan), using Cu Kα radiation. X-ray photoelectron spectroscopy (XPS) analysis was carried out on a RBD-upgraded PHI-5000C ESCA system (Perkin Elmer) with Mg Kα radiation ($h\nu$ = 1253.6 eV). Binding energies were calibrated with containment carbon (C1s = 284.6 eV). The specific surface area of the powders was determined by nitrogen absorption (BET, ASAP 2020M Analyzer, Micromeritics). UV–vis diffuse reflectance spectra (DRS) were recorded on a UV-2401 Shimadzu spectrometer.

### 2.3. Photocatalytic reactions and analysis

Experiments were carried out in a photoreaction apparatus, which is shown in Fig. 1. The apparatus consists of two parts. The first part is an annular quartz tube and cooling water passes through an inner thimble of the annular tube. In the axial center of the reactor, there is a 500W xenon lamp as the light source. The wavelength of the visible light is controlled through a 400 nm cut filter. The second part is a 50 mL quartz tube, which is put on a magnetic stirrer. The reaction solution in the quartz tube was stirred during the experiments. The distance between the light source and the surface of the reaction solution is 4 cm.

In the experiment, the solution of atrazine was put into the quartz tube at first, of which pH was adjusted to 2.6 with $H_2SO_4$ solution ($V_{H_2SO_4} : V_{\text{deionized water}} = 1 : 20$). Then $Fe^{3+}$ stock solution (pH 2.6) and 0.03 g tantalum (oxy)nitrides were put into the tube. To achieve an adsorption/desorption equilibrium of $Fe^{3+}$ and atrazine on the surface of the tantalum (oxy)nitrides, the suspension was kept in the dark and stirred for 30 min. After that, the stock solution of $H_2O_2$ was put into the tube and at the same time the lamp was turned on to initiate the photoreaction. The samples were taken out at the desired time intervals and filtered with a 0.22 μm Millipore filter to remove the catalyst. In the experiment of $Fe^{3+}$ photoreduction, the procedure was similar except that no atrazine and $H_2O_2$ was added.

Analysis of atrazine was conducted on an Agilent 1120 compact HPLC system with a reversed phase C 18 column and UV detector. The UV detector wavelength was set at 235 nm. The mobile phase was 70:30 (v/v) of methanol and deionized water with a flow rate of 1.0 mL/min. The potential reaction of atrazine with hydroxyl radical was prevented by adding 1.0 mL of 1.0 M *tert*-butyl alcohol to the sample.

The concentration of $Fe^{2+}$ was measured by the *o*-phenanthroline colorimetric method ($\lambda$ = 510 nm, $\varepsilon = 1.1 \times 10^4\ M^{-1}\ cm^{-1}$) [24]. The concentration of $H_2O_2$ was

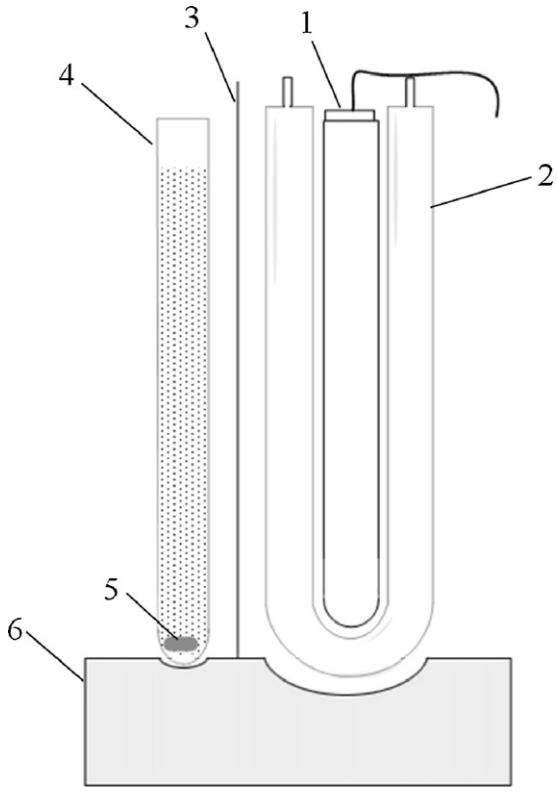


**Fig. 1.** Schematic diagram of the experimental set-up: 1. Lamp, 2. Water-cooled jacket, 3. 400 nm cut filter, 4. Quartz tube, 5. Magneton, 6. Magnetic stirrer.

determined by a spectrophotometric analysis using the potassium titanium (IV) oxalate method [25].

## 3. Results and discussion

### 3.1. Characterisation of tantalum (oxy)nitride samples

#### 3.1.1. XPS analysis of tantalum (oxy)nitrides

XPS analysis was used to determine the composition of the tantalum (oxy)nitride samples. Table 1 summarizes the ratios of Ta:O:N in the tantalum (oxy)nitride samples prepared under different conditions. The content of nitrogen in the tantalum (oxy)nitride samples increased with increasing nitridation temperature, nitridation time and flow rate of $NH_3$. Within the range adopted in this study, the effects of nitridation temperature and nitridation time on the nitrogen content of the samples are significant. At nitridation temperatures of 600, 700 and 800 °C (in a 0.3 L/min $NH_3$ flow for 6 h), the ratios of N to O were 9.7%, 43.0% and 71.3%, respectively. The ratios of N to O were 7.2%, 43.0% for the nitridation times of 2 and 4 h, respectively (at 700 °C in a 0.3 L/min $NH_3$ flow). While the effect of $NH_3$ flow rate was relatively slight. The ratios of N to O were 30.6% and 43.0% at $NH_3$ flow rates of 0.1 and 0.3 L/min, respectively (at 700 °C for 6 h).

Fig. 2(a) and (b) shows the O1s and N1s XPS spectra of $Ta_2O_5$ and the samples produced at the nitridation temperatures of 600, 700 and 800 °C, respectively. The peak positions of the O1s and N1s spectra were very similar in all samples. While the peak areas of O1s and N1s changed in opposite, as the areas assigned to O1s decreased with nitridation temperature, and the areas assigned to N1s increased. Fig. 2(c) was the typical simulation of N1s peaks (sample 9 as an example). As could be seen, the N1s peak consisted of the peak with the binding energy of 395.67 eV, which was generally considered to be the evidence for the presence of Ta–N bonds when N atoms replace O atoms in $Ta_2O_5$ crystal lattices [19]. The

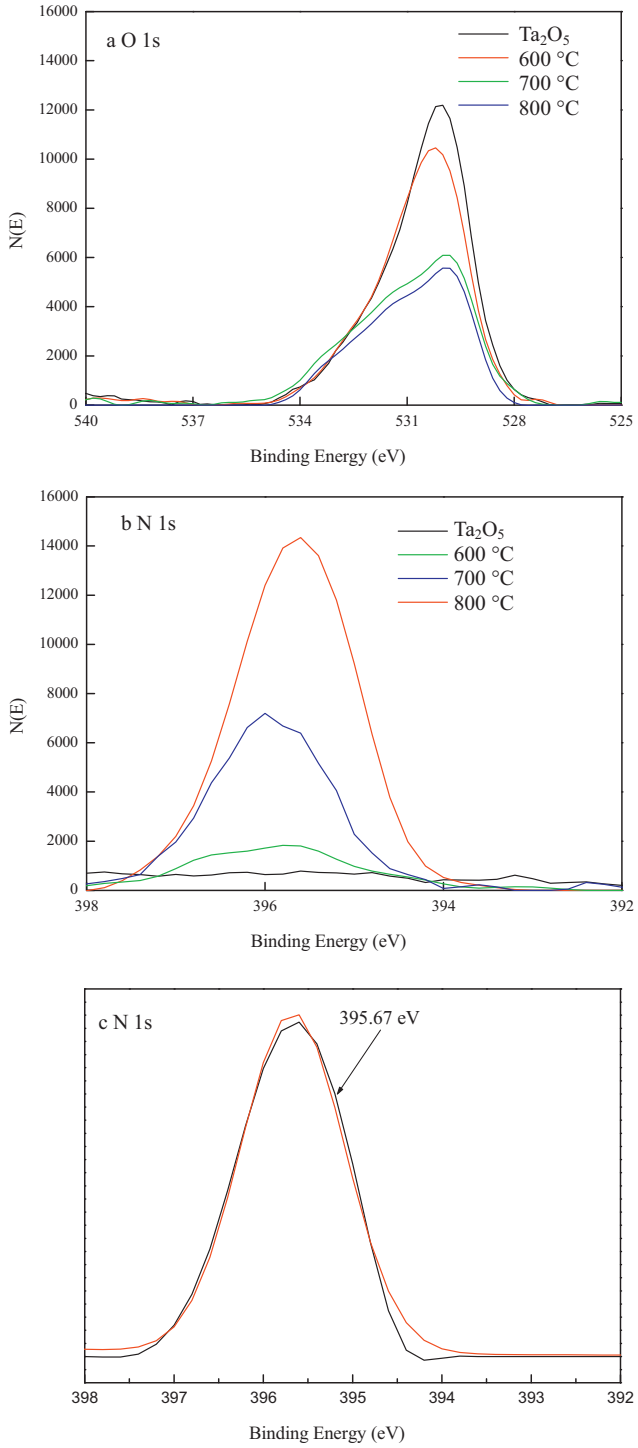


**Fig. 2.** O1s (a) and N1s (b) XPS spectra of $Ta_2O_5$ and the tantalum (oxy)nitride samples prepared at 600, 700 and 800 °C for 6 h at a flow rate of 0.3 L/min for $NH_3$; N1s (c) simulation of sample 9 (preparation conditions: temperature = 800 °C, $Q_{NH_3}$ = 0.3 L/min, time = 6 h).

replacement of the N atom by an O atom results in the band gap narrowing and a red shift of absorption for the tantalum (oxy)nitride samples [26,27]. Higher nitrogen content leads to a narrower band gap and stronger optical absorption in visible light domain.

#### 3.1.2. XRD and DRS analyses

The nitridation reaction of $Ta_2O_5$ always leads to the formation of the mixture of TaON and $Ta_3N_5$. Fig. 3 depicts the XRD

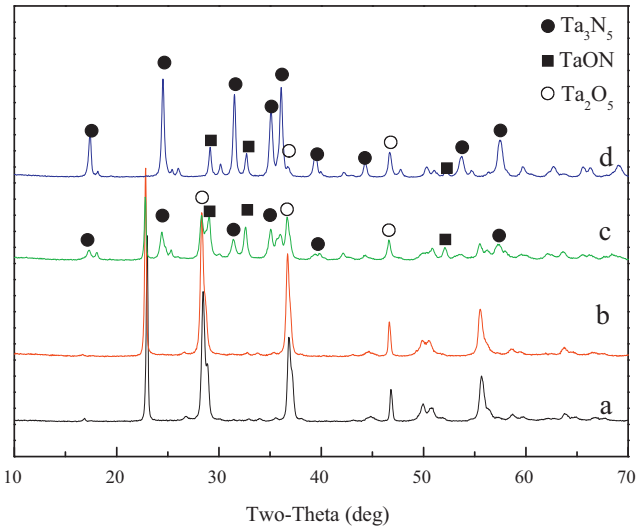


**Fig. 3.** XRD patterns of $Ta_2O_5$ (a) and tantalum (oxy)nitride samples prepared at 600 °C (b), 700 °C (c) and 800 °C (d).

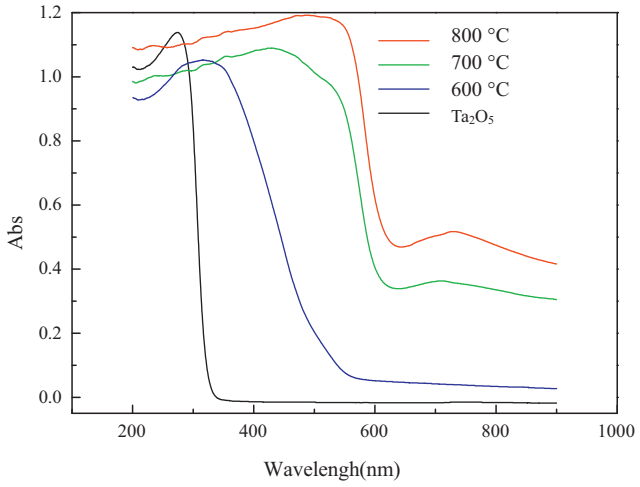


**Fig. 4.** UV–vis diffuse reflectance absorption spectra of $Ta_2O_5$ and tantalum (oxy)nitride samples prepared at 600, 700 and 800 °C for 6 h at the $NH_3$ flow rate of 0.3 L/min.

patterns of $Ta_2O_5$ and tantalum (oxy)nitride samples prepared at 600, 700 and 800 °C for 6 h at a $NH_3$ flow rate of 0.3 L/min. The XRD patterns showed that reaction temperature had a significant effect on the nitridation of $Ta_2O_5$. With a nitridation temperature as low as 600 °C, the colour of $Ta_2O_5$ changed to yellow, indicating that the nitridation reaction was starting. However, almost none of the crystalline phase of TaON and $Ta_3N_5$ was detected by XRD. The samples which were prepared at 700 °C and 800 °C both consisted of $Ta_2O_5$, TaON and $Ta_3N_5$. Compared to the sample prepared at 700 °C, stronger diffraction peaks corresponding to $Ta_3N_5$ and weaker peaks assigned to TaON appeared in the sample prepared at 800 °C. During the nitridation process, tantalum in the oxidation state V can form two ionic-covalent nitride types, $Ta_3N_5$ and TaON. TaON is regarded as the intermediate between the oxide precursor of $Ta_2O_5$ and the fully nitrided phase of $Ta_3N_5$ [28]. As the reaction of $Ta_2O_5$ with $NH_3$ to form TaON and $Ta_3N_5$ is endothermic [29], the content of nitrogen increased with the nitridation temperature.

The colours of samples prepared at 600, 700 and 800 °C are yellow, orange and red, respectively. Fig. 4 shows the UV–vis diffuse reflectance spectra of tantalum (oxy)nitride samples prepared at 600, 700 and 800 °C for 6 h in the $NH_3$ flow rate of 0.3 L/min. The UV–vis diffuse reflectance spectrum of $Ta_2O_5$ is also shown. Compared with the absorption spectrum of $Ta_2O_5$, the tantalum (oxy)nitride samples showed an obvious red shift with a stronger absorption in the wavelength range from 400 to 800 nm. When the nitridation temperature increased, a further red shift and a stronger absorption of the tantalum (oxy)nitride samples were observed. Samples obtained at 600, 700 and 800 °C showed absorption edges of approximately 520 nm, 620 nm and 640 nm, respectively, while the absorption edge of $Ta_2O_5$ was approximately 330 nm. According to the theoretical calculation, $Ta_3N_5$ and TaON show band gaps at 2.08 eV and 2.4 eV, respectively [19,30]. The strongest optical absorption of the sample prepared at 800 °C was mainly attributed to the highest content of $Ta_3N_5$.

### 3.1.3. BET analysis

BET surface areas of the samples are also given in Table 1. From Table 1, the surface areas of the samples obtained at 600 °C decreased compared to that of the precursor of $Ta_2O_5$ (2.965 $m^2/g$). Since little tantalum (oxy)nitrides was formed at 600 °C, the decrease of the surface area might be due to the sintering of $Ta_2O_5$ particles at the high temperature. The specific surface area of the sample obtained at 700 °C was largest compared to those at 600 °C and 800 °C (in a $NH_3$ flow rate of 0.3 L/min for 6 h). XRD results showed that the contents of TaON followed 700 °C > 800 °C > 600 °C and the contents of $Ta_3N_5$ were 800 °C > 700 °C > 600 °C. Combined the results of XRD with BET, it may be included that the surface areas were TaON > $Ta_3N_5$ > $Ta_2O_5$.

## 3.2. Photocatalytic activity of tantalum (oxy)nitrides

### 3.2.1. Photocatalytic activity of tantalum (oxy)nitrides for $Fe^{3+}$ reduction

Prior to the investigation into the photocatalytic activity of tantalum (oxy)nitrides, the adsorption of $Fe^{3+}$, $H_2O_2$ and atrazine on the samples was investigated; little adsorption was observed.

Table 1 also lists the generation of $Fe^{2+}$ in $Fe^{3+}$ solution after 180 min of irradiation with visible light with the addition of tantalum (oxy)nitride. It is interesting to find that the ability of tantalum (oxy)nitrides to reduce $Fe^{3+}$ was apparently not determined by the nitrogen content and the absorption under visible light domain. The highest concentration of $Fe^{2+}$ was achieved in the presence of sample 7 (preparation conditions: temperature = 700 °C, $Q_{NH_3}$ = 0.3 L/ min, time = 6 h). The amount of $Fe^{2+}$ generated in the presence of sample 7 was approximately 1.7 times the amount generated with sample 9. However, sample 9 has a higher nitrogen content and stronger visible light absorption.

XRD results showed that more TaON was contained in sample 7 and when the nitridation temperature increased to 800 °C (sample 9), some TaON changed to $Ta_3N_5$. Here we tried to compare the photocatalytic activity of TaON and $Ta_3N_5$ for $Fe^{3+}$ reduction under visible light irradiation as such information is limited.

Firstly, the following two nitridation processes were conducted to obtain the pure TaON and pure $Ta_3N_5$. Based on the previous reports [19,31,32], $Ta_2O_5$ was nitrided at 750 °C in a 0.06 L/min $NH_3$ flow for 12 h and at 850 °C in a 0.9 L/min $NH_3$ flow for 12 h to form TaON (sample 12) and $Ta_3N_5$ (sample 13), respectively. The XRD patterns of sample 12 and sample 13 are shown in Fig. 5. As could be seen, sample 13 was almost the pure $Ta_3N_5$ and the majority of sample 12 was TaON.

The photoreduction of $Fe^{3+}$ under visible light irradiation for 3 h by sample 12, sample 13 and a mixture of sample 12 and sample 13 (w:w = 1:1) were investigated.

The reduction of $Fe^{3+}$ over sample 12 (2.34 mg/L of $Fe^{3+}$ formed after 3 h visible light irradiation) was significantly faster than that over sample 13 (1.03 mg/L of $Fe^{3+}$ formed after 3 h visible light irradiation). It is concluded that the ability of TaON to reduce $Fe^{3+}$ is

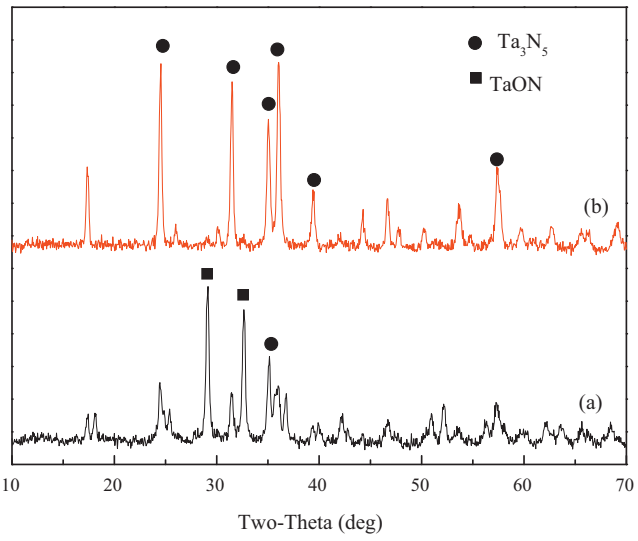


**Fig. 5.** XRD patterns of sample 12 (a) (nitrided at 750 °C in a 0.06 L/min $NH_3$ flow for 12 h) and sample 13 (b) (at 850 °C in a 0.9 L/min $NH_3$ flow for 12 h).

higher than that of $Ta_3N_5$. In the presence of the mixture of sample 12 and sample 13, there was 1.91 mg/L of $Fe^{2+}$ formed, a little higher than 1.69 mg/L (the average of 2.34 mg/L and 1.03 mg/L). This may be due to the synergism between TaON and $Ta_3N_5$ for the photoreduction of $Fe^{3+}$.

TaON and $Ta_3N_5$ have been reported as the visible-light photocatalyst to decompose water to $H_2$ and $O_2$. It was also found that the reduction of $H^+$ to $H_2$ over TaON was higher than over $Ta_3N_5$ [31]. The difference of the photocatalytic activity between TaON and $Ta_3N_5$ is similar to that of the two phases of $TiO_2$, anatase and rutile. Anatase has a band gap of 3.2 eV, while rutile has a smaller band gap of 3.0 eV. Nevertheless, anatase is generally regarded as the more photochemically active phase of $TiO_2$, presumably due to the combined effect of lower rates of recombination and higher surface adsorptive capacity [33]. In addition, the mixing of an active phase (anatase) with a comparatively inactive phase (rutile) produces a class of photocatalysts with higher activity [34,35].

The BET results showed that sample 12 has higher specific surface area (10.052 $m^3$/g) than sample 13 (6.731 $m^3$/g), which could be one of the reasons for the higher photocatalytic activity of TaON. Other factors to influence the photocatalytic activity of TaON and $Ta_3N_5$ need exhaustive investigation in the further work.

### *3.2.2. Enhancement of Fenton reaction and atrazine degradation by tantalum (oxy)nitrides*

Fig. 6(a) shows the generation of $Fe^{2+}$ by various systems under visible light. No $H_2O_2$ was added in these systems. Little ferrous ion was generated in $Fe^{3+}$ solution either without catalyst or with $Ta_2O_5$. With the addition of sample 7, $Fe^{2+}$ was produced continuously under the irradiation of visible light and then slowed down. After 180 min of irradiation, more than 2 mg/L of $Fe^{2+}$ had been produced.

In the presence of $H_2O_2$, the generated $Fe^{2+}$ could decompose $H_2O_2$ to •OH. Fig. 6(b) shows the decomposition of $H_2O_2$ in a photo-Fenton-like system, a photo-Fenton-like system with $Ta_2O_5$ (called photo-Fenton-like-$Ta_2O_5$ system) and a photo-Fenton-like system with tantalum (oxy)nitride (sample 7) (called photo-Fenton-like-tantalum (oxy)nitride system) under visible light. In the systems of photo-Fenton-like and photo-Fenton-like-$Ta_2O_5$, the decomposition of $H_2O_2$ was very slow, only 20–30% of $H_2O_2$ was consumed after 180 min. The decomposition of $H_2O_2$ in these two systems was due to Eqs. (1) and (3). $Fe^{3+}$ firstly reacted with $H_2O_2$ to generate $Fe^{2+}$ at a very slow rate of 0.01–0.001 $M^{-1}$ $s^{-1}$, and then $Fe^{2+}$

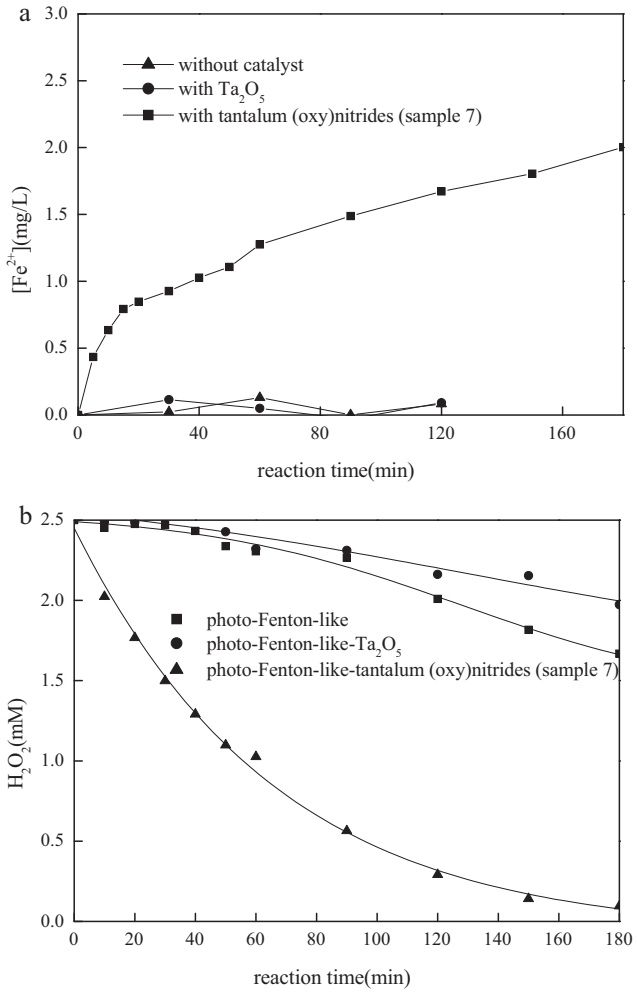


**Fig. 6.** Reduction of $Fe^{3+}$ (a) and decomposition of $H_2O_2$ (b) in various systems under visible light: $[Fe^{3+}]_0$ = 28 mg/L, $[H_2O_2]_0$ = 2.5 mM, input of tantalum (oxy)nitride = 0.6 g/L, pH 2.6.

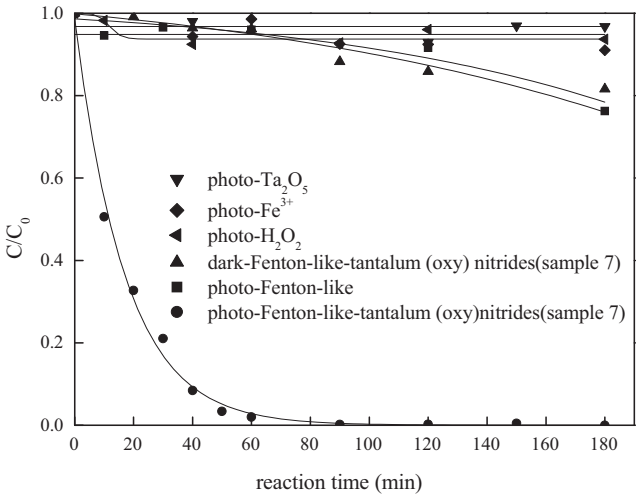


**Fig. 7.** Degradation of atrazine in various systems under visible light: $[Fe^{3+}]_0$ = 28 mg/L, $[H_2O_2]_0$ = 2.5 mM, $[atrazine]_0$ = 18 mg/L, input of tantalum (oxy)nitride = 0.6 g/L, pH 2.6.

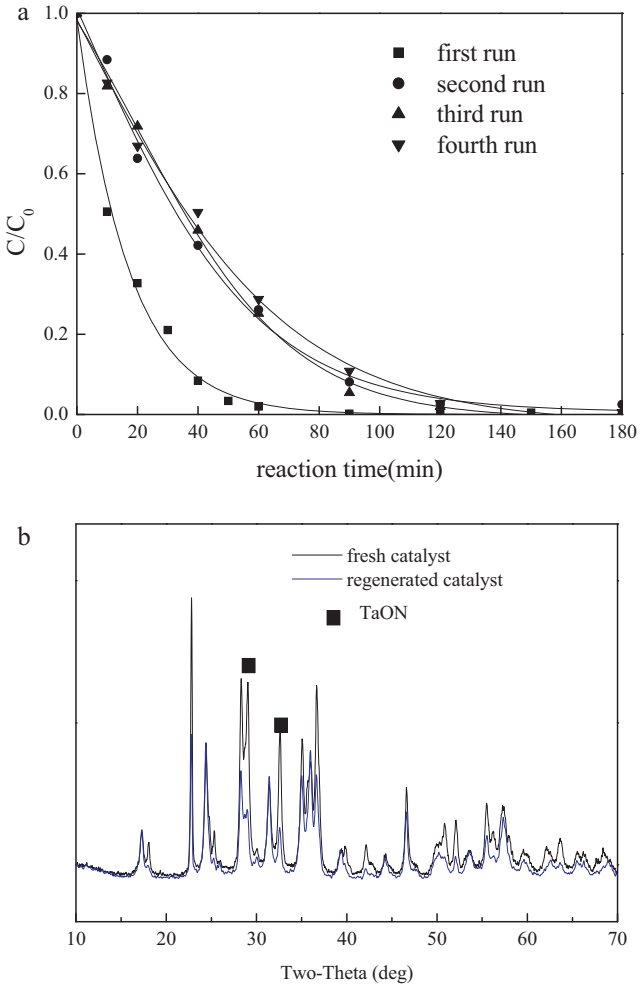


**Fig. 8.** (a) Degradation of atrazine over the fresh and regenerated tantalum (oxy)nitride samples in photo-Fenton-like system for four experimental runs (b) XRD patterns of a fresh and a regenerated samples: $[Fe^{3+}]_0$ = 28 mg/L, $[atrazine]_0$ = 18 mg/L, input of tantalum (oxy)nitride = 0.6 g/L, pH 2.6.

catalyzed $H_2O_2$ to •OH and was oxidized to $Fe^{3+}$. A cycling of $Fe^{2+}/Fe^{3+}$ was established, with slow decomposition of $H_2O_2$. In the system of photo-Fenton-like-tantalum (oxy)nitrides (sample 7), more than 96% of $H_2O_2$ was decomposed after 180 min. This is due to the enhancement of $Fe^{3+}$ reduction by the tantalum (oxy)nitrides.

The enhancement of the photo-Fenton-like degradation of contaminants by tantalum (oxy)nitrides under visible light was also investigated. Atrazine was chosen as a target pollutant because atrazine has no absorption under visible light. Because atrazine or the intermediates of atrazine cannot interact with $Fe^{3+}/Fe^{2+}$, which was different to aromatic compounds [36], the generation of $Fe^{2+}$ during the degradation of atrazine could be regarded solely as the role of tantalum (oxy)nitrides.

Fig. 7 shows the changes in atrazine concentration in different systems under visible light. Atrazine scarcely underwent direct photolysis (data no shown). In systems where only $Fe^{3+}$ or $Ta_2O_5$ was added, little degradation of atrazine was observed under visible light. In the presence of tantalum (oxy)nitrides and $H_2O_2$, atrazine could hardly be degraded. In the process of dark-Fenton-like-tantalum (oxy)nitrides, approximately 19% of the atrazine was degraded after 3 h reaction. In the process of photo-Fenton-like, the trend of atrazine degradation is similar to that of dark-Fenton-like-tantalum (oxy)nitrides. In these two systems, $Fe^{3+}$ was slowly reduced to $Fe^{2+}$ through $H_2O_2$ (Eq. (3)). And then the Fenton reaction (Eq. (1)) produced •OH, resulting in a slight degradation of atrazine. With the addition of tantalum (oxy)nitrides (sample 7), the degradation of atrazine in a photo-Fenton-like system was obviously enhanced. After 120 min of irradiation with visible light, atrazine was degraded completely.

### 3.2.3. *Reusability of tantalum (oxy)nitrides photocatalyst*

Fig. 8(a) shows the reusability of the tantalum (oxy)nitrides (sample 7) in photo-Fenton-like system during four experimental runs. As could be seen, the degradation of atrazine in the second run was slower than that in the first run. Compared with that over the fresh catalyst, the percentage of atrazine degradation decreased by about 25% at 60 min and 8% at 90 min in the second run. Nevertheless, almost all atrazine was also removed after 120 min in the second run. In addition, it was encouraging that the degradation rate of atrazine was almost the same in the second, third and fourth runs.

The XRD patterns of a fresh catalyst sample and a regenerated catalyst sample are compared in Fig. 8(b). The two XRD patterns was similar except that the peaks corresponding to TaON at $2\theta$ of 29.0 and 32.6° were a little lower in the regenerated catalyst. When the fresh tantalum (oxy)nitrides catalyst was subjected to the photo-Fenton-like system in the first run, the component of the catalyst changed a little and the photocatalytic activity decreased. But after that, the tantalum (oxy)nitrides catalyst became stable and showed good activity for atrazine degradation.

## 4. Conclusion

Tantalum (oxy)nitrides were prepared by the nitridation of $Ta_2O_5$ at 600–800 °C in a $NH_3$ rate of 0.1–0.5 L/min for 2–6 h. XPS analysis showed that the degree of nitridation was significantly affected by the nitridation temperature and the nitridation time. The N1s XPS spectra confirmed the replacement of O atoms by N atoms to form Ta–N bonds in the $Ta_2O_5$ crystal lattice. With the increase of the nitridation temperature, $Ta_2O_5$ was converted into TaON and then to $Ta_3N_5$. DRS analysis showed that the tantalum (oxy)nitride samples prepared at 600, 700 and 800 °C possessed absorption edges around 520, 620 and 640 nm, respectively. But the ability of the tantalum (oxy)nitride samples to reduce $Fe^{3+}$ did not increase continuously with the nitrogen content and the absorption range under visible light. The generation of $Fe^{2+}$ in the presence of sample 7 (nitrided at 700 °C) was approximately 1.7 times that generated with sample 9 (nitrided at 800 °C). This was because the photoactivity for $Fe^{3+}$ reduction of TaON is much higher than $Ta_3N_5$.

With the addition of sample 7, $H_2O_2$ was efficiently decomposed to generate hydroxyl radicals in a photo-Fenton-like system under visible light. The degradation of atrazine was significantly accelerated and almost all atrazine was degraded completely after 120 min. The regenerated tantalum (oxy)nitrides catalyst became stable after the first run and showed good activity for atrazine degradation.

## Acknowledgements

The authors would like to acknowledge financial support for this work provided by the National Science Foundation of China (No. 20906098), the National Science Foundation of Jiangsu Province, China (No. BK2010602), the Foundation of Director of Nanjing Institute of Geography and Limnology, Chinese Academy of China (No. NIGLAS2010QD03) and the State Key Laboratory of Hydrology—Water Resources and Hydraulic Engineering, Hohai University (No. 2009490811).

## References


[1] W. Chu, C.Y. Kwan, K.H. Chan, S.K. Kam, A study of kinetic modelling and reaction pathway of 2,4-dichlorophenol transformation by photo-Fenton-like oxidation, J. Hazard. Mater. 121 (1–3) (2005) 119–126.

[2] I. Arslan-Alaton, G. Tureli, T. Olmez-Hanci, Treatment of azo dye production wastewaters using photo-Fenton-like advanced oxidation processes: optimization by response surface methodology, J. Photochem. Photobiol. A: Chem. 202 (2–3) (2009) 142–153.

[3] T.M. Elmorsi, Y.M. Riyad, Z.H. Mohamed, H.M.H. Abd El Bary, Decolorization of Mordant red 73 azo dye in water using $H_2O_2$/UV and photo-Fenton treatment, J. Hazard. Mater. 174 (1–3) (2009) 352–358.

[4] M. Jiménez, I. Oller, M.I. Maldonado, S. Malato, A. Hernández-Ramírez, A. Zapata, J.M. Peralta-Hernández, Solar photo-Fenton degradation of herbicides partially dissolved in water, Catal. Today 161 (1) (2011) 214–220.

[5] S. Navarro, J. Fenoll, N. Vela, E. Ruiz, G. Navarro, Removal of ten pesticides from leaching water at pilot plant scale by photo-Fenton treatment, Chem. Eng. J. 167 (1) (2011) 42–49.

[6] M.R.A. Silva, W. Vilegas, M.V.B. Zanoni, R.F. Pupo Nogueira, Photo-Fenton degradation of the herbicide tebuthiuron under solar irradiation: iron complexation and initial intermediates, Water Res. 44 (12) (2010) 3745–3753.

[7] M. Pera-Titus, V. Garcia-Molina, M.A. Banos, J. Gimenez, S. Esplugas, Degradation of chlorophenols by means of advanced oxidation processes: a general review, Appl. Catal. B: Environ. 47 (4) (2004) 219–256.

[8] C. Walling, Fenton's reagent revisited, Accounts Chem. Res. 8 (4) (1975) 125–131.

[9] A. Safarzadeh-Amiri, J.R. Bolton, S.R. Cater, The use of iron in advanced oxidation processes, J. Adv. Oxid. Technol. 1 (1996) 18–26.

[10] L.G. Devi, B.N. Murthy, S.G. Kumar, Heterogeneous photo catalytic degradation of anionic and cationic dyes over $TiO_2$ and $TiO_2$ doped with $Mo^{6+}$ ions under solar light: correlation of dye structure and its adsorptive tendency on the degradation rate, Chemosphere 76 (8) (2009) 1163–1166.

[11] B. Tryba, A.W. Morawski, M. Inagaki, M. Toyoda, Effect of the carbon coating in Fe–C–$TiO_2$ photocatalyst on phenol decomposition under UV irradiation via photo-Fenton process, Chemosphere 64 (7) (2006) 1225–1232.

[12] Z. Wang, C. Chen, F. Wu, B. Zou, M. Zhao, J. Wang, C. Feng, Photodegradation of rhodamine B under visible light by bimetal codoped $TiO_2$ nanocrystals, J. Hazard. Mater. 164 (2–3) (2009) 615–620.

[13] J. Sato, N. Saito, Y. Yamada, K. Maeda, T. Takata, J.N. Kondo, M. Hara, H. Kobayashi, K. Domen, Y. Inoue, $RuO_2$-loaded β-$Ge_3N_4$ as a non-oxide photocatalyst for overall water splitting, J. Am. Chem. Soc. 127 (12) (2005) 4150–4151.

[14] J. Ananpattarachai, P. Kajitvichyanukul, S. Seraphin, Visible light absorption ability and photocatalytic oxidation activity of various interstitial N-doped $TiO_2$ prepared from different nitrogen dopants, J. Hazard. Mater. 168 (1) (2009) 253–261.

[15] X.-Z. Shen, Z.-C. Liu, S.-M. Xie, J. Guo, Degradation of nitrobenzene using titania photocatalyst co-doped with nitrogen and cerium under visible light illumination, J. Hazard. Mater. 162 (2–3) (2009) 1193–1198.

[16] A. Ghicov, J.M. Macak, H. Tsuchiya, J. Kunze, V. Haeublein, L. Frey, P. Schmuki, Ion implantation and annealing for an efficient N-doping of $TiO_2$ nanotubes, Nano Lett. 6 (5) (2006) 1080–1082.

[17] X. Wang, T.-T. Lim, Effect of hexamethylenetetramine on the visible-light photocatalytic activity of C–N codoped $TiO_2$ for bisphenol A degradation: evaluation of photocatalytic mechanism and solution toxicity, Appl. Catal. A: Gen. 399 (1–2) (2011) 233–241.

[18] V.M. Menéndez-Flores, D.W. Bahnemann, T. Ohno, Visible light photocatalytic activities of S-doped $TiO_2$–$Fe^{3+}$ in aqueous and gas phase, Appl. Catal. B: Environ. 103 (1–2) (2011) 99–108.

[19] W.-J. Chun, A. Ishikawa, H. Fujisawa, T. Takata, J.N. Kondo, M. Hara, M. Kawai, Y. Matsumoto, K. Domen, Conduction and valence band positions of $Ta_2O_5$, TaON, and $Ta_3N_5$ by UPS and electrochemical methods, J. Phys. Chem. B 107 (8) (2003) 1798–1803.

[20] Q.H. Zhang, L. Gao, $Ta_3N_5$ nanoparticles with enhanced photocatalytic efficiency under visible light irradiation, Langmuir 20 (22) (2004) 9821–9827.

[21] R. Abe, M. Higashi, K. Domen, Facile fabrication of an efficient oxynitride TaON photoanode for overall water splitting into $H_2$ and $O_2$ under visible light irradiation, J. Am. Chem. Soc. 132 (34) (2010) 11828–11829.

[22] X. Feng, T.J. LaTempa, J.I. Basham, G.K. Mor, O.K. Varghese, C.A. Grimes, $Ta_3N_5$ nanotube arrays for visible light water photoelectrolysis, Nano Lett. 10 (3) (2010) 948–952.

[23] Y.F. Wang, W.H. Ma, C.C. Chen, X.F. Hu, J.C. Zhao, J.C. Yu, $Fe^{3+}$/$Fe^{2+}$ cycling promoted by $Ta_3N_5$ under visible irradiation in Fenton degradation of organic pollutants, Appl. Catal. B: Environ. 75 (3–4) (2007) 256–263.

[24] H. Tamura, K. Goto, T. Yotsuyanagi, M. Nagayama, Spectrophotometric determination of iron(II) with 1,10-phenanthroline in the presence of large amounts of iron(III), Talanta 21 (4) (1974) 314–318.

[25] R.M. Sellers, Spectrophotometric determination of hydrogen peroxide using potassium titanium(IV) oxalate, Analyst 150 (1980) 950–954.

[26] G. Hitoki, T. Takata, J.N. Kondo, M. Hara, H. Kobayashi, K. Domen, An oxynitride, TaON, as an efficient water oxidation photocatalyst under visible light irradiation (≤500 nm), Chem. Commun. 16 (2002) 1698–1699.

[27] I. Tsuji, H. Kato, H. Kobayashi, A. Kudo, Photocatalytic $H_2$ evolution reaction from aqueous solutions over band structure-controlled $(AgIn)_xZn_{2(1-x)}S_2$ solid solution photocatalysts with visible-light response and their surface nanostructures, J. Am. Chem. Soc. 126 (41) (2004) 13406–13413.

[28] W.R. Matizamhuka, I. Sigalas, M. Herrmann, Synthesis, sintering and characterisation of TaON materials, Ceram. Int. 34 (6) (2008) 1481–1486.

[29] E. Orhan, F. Tessier, R. Marchand, Synthesis and energetics of yellow TaON, Solid State Sci. 4 (8) (2002) 1071–1076.

[30] C.M. Fang, E. Orhan, G.A. de Wijs, H.T. Hintzen, R.A. de Groot, R. Marchand, J.Y. Saillard, G. de With, The electronic structure of tantalum (oxy)nitrides TaON and $Ta_3N_5$, J. Mater. Chem. 11 (4) (2001) 1248–1252.

[31] T. Takata, G. Hitoki, J. Kondo, M. Hara, H. Kobayashi, K. Domen, Visible-light-driven photocatalytic behavior of tantalum-oxynitride and nitride, Res. Chem. Intermediat. 33 (1) (2007) 13–25.

[32] T. Hisatomi, M. Otani, K. Nakajima, K. Teramura, Y. Kako, D. Lu, T. Takata, J.N. Kondo, K. Domen, Preparation of crystallized mesoporous $Ta_3N_5$ assisted by chemical vapor deposition of tetramethyl orthosilicate, Chem. Mater. 22 (13) (2010) 3854–3861.

[33] D.C. Hurum, A.G. Agrios, K.A. Gray, T. Rajh, M.C. Thurnauer, Explaining the enhanced photocatalytic activity of Degussa P25 mixed-phase $TiO_2$ using EPR, J. Phys. Chem. B 107 (19) (2003) 4545–4549.

[34] D.C. Hurum, K.A. Gray, T. Rajh, M.C. Thurnauer, Recombination pathways in the Degussa P25 formulation of $TiO_2$: surface versus lattice mechanisms, J. Phys. Chem. B 109 (2) (2004) 977–980.

[35] T. Ohno, K. Tokieda, S. Higashida, M. Matsumura, Synergism between rutile and anatase $TiO_2$ particles in photocatalytic oxidation of naphthalene, Appl. Catal. A: Gen. 244 (2) (2003) 383–391.

[36] Y. Du, M. Zhou, L. Lei, Role of the intermediates in the degradation of phenolic compounds by Fenton-like process, J. Hazard. Mater. 136 (3) (2006) 859–865.